Microelectronics Reliability xxx (xxxx) xxxx

Contents lists available at ScienceDirect

Microelectronics Reliability

journal homepage: www.elsevier.com/locate/microrel

Magnetic field imaging and light induced capacitance alteration for failure analysis of Cu-TSV interconnects

Ingrid De Wolf[a,b,*], Kristof J.P. Jacobs[b], Antonio Orozco[c]

[a] Dept. Materials Engineering, KULeuven, Belgium
[b] imec, Remisebosweg 1, 3001 Leuven, Belgium
[c] Neocera, LLC, Beltsville MD, USA

A B S T R A C T

This paper discusses Cu-filled Through Silicon Via (TSV) failure analysis cases where known FA methods were used in an alternative way. Results are shown using magnetic field imaging (MFI) on a cross-sectioned chip to detect a leakage current path, and MFI and Light Induced Capacitance Alteration (LICA) to detect opens in TSV daisy chains.

1. Introduction

The vertical electrical interconnection between different functional layers in 3D technology is commonly made by Through Si Vias (TSVs) [1]. Depending on the application, these TSVs can have lengths ranging from 100 μm down to a few μm. The diameter generally scales accordingly. These TSVs are indispensable for 3D technology, ensuring shorter electrical interconnections and thus allowing a higher device densification and signal speed. But they are also susceptible to failure. There are several potential failure causes and effects in TSVs [2], such as voids (electromigration or processing induced), delamination, misalignment, bad connection to metals, shorts or opens in the connection between TSVs, liner breakdown, stress induced effects, etc. In this paper, we discuss alternative uses of two known failure analysis techniques, magnetic field imaging (MFI) and Light Induced Capacitance Alteration (LICA), to detect TSV failures related to liner breakdown (BD) induced leakage and opens in metals connecting TSVs.

2. Leakage path between TSVs

Magnetic field imaging uses a scanning magnetic sensor (SQUID, GMR or TMR) to detect the magnetic field associated with the signal in the device [3]. The acquired magnetic field data are then converted into current or RF signal density using an inverse problem algorithm [4] to locate the current path and any defects (shorts, opens) associated with it. We investigated whether this technique can be used to detect the position of a leakage current path that was measured between TSVs, and its cause.

The failed sample is a thinned Si wafer glued on a carrier wafer, containing several 100 μm long Cu TSVs, 10 μm diameter. They are grouped by fives, connecting at the top and bottom on a Cu redistribution layer (RDL) in the shape of a cross, as shown in Fig. 1a. The crosses are electrically isolated from each other. Fig. 1b shows a cross-section schematic view.

During wafer level testing, a short resulting in a leakage current was measured between Cross 1 and Cross 3 in some chips of the wafer. Most of the tested chips have a leakage current < 1 nA at 20 V, which was considered normal, but some had a higher leakage indicating a failure. The failure analysis question was: Where is the location of this leakage path and what is the cause. This path can for example be located at the surface, or at the bottom, of the Si chip (see Fig. 1b). A chip with a leakage current between cross 1 and 3 of 110 nA at 20 V was selected for failure analysis. If TSV liner breakdown would be the cause of this short, photon emission microscopy (PEM) could be considered to identify the breakdown position [5]. However, it cannot locate the path of a leakage current, and in this sample, the Cu RDL layer and the fact that it covers 5 connected TSVs would make location of the failed TSV complicated. In addition, a leakage current does not necessarily go together with photon emission, especially if the problem would be in the metallization. And if the problem is located underneath the RDL metal, it will block photons from passing and thus either prevent its detection or go through transparent areas that may not coincide with the actual location of the failure. Similar considerations hold for OBIRCH, thermal imaging, LIVA and LICA. For this reason, it was considered to use MFI. The magnetic field passes unaffected through the different layers, not hindered by the RDL. MFI can detect the location of a current path, even for low currents, and can provide depth information [6,7]. Another option to obtain depth information would be

* Corresponding author.
E-mail address: ingrid.dewolf@imec.be (I. De Wolf).

https://doi.org/10.1016/j.microrel.2020.113780
Received 28 May 2020; Accepted 10 July 2020

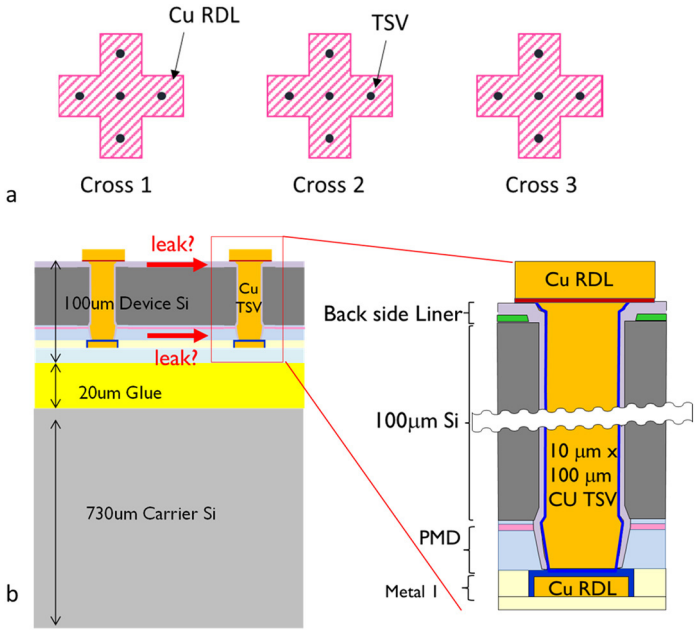

Fig. 1. a. Top view of the 3 RDL crosses. The black dots indicate the position of TSVs (5/cross). b. Cross-section view.

attempting MFI from the cross-section. If feasible, this option could offer a future solution for FA on samples where optical techniques cannot be used.

First an MFI-image was measured as conventionally done, from the top-side of the sample. Probe 1 was placed on Cross 1 and 0 V was applied. Probe 2 was placed on Cross 3 and 5 V was applied (see Fig. 2). No meaningful MFI signal could be obtained from the top side of the sample. This indicates that the leakage path is most likely located near the bottom side of the 100 µm thick Si. Indeed, as the leakage current is low, a large distance from the current path to the sensor makes the intensity of the field weak, and no discernible signal can be detected. Scanning on the cross-section side is one way to reduce the separation distance and it could allow us to see the leakage path.

So, next, MFI was done on the cross-section of the sample, thus reducing in principle the distance between current and sensor. The cross-sectioning was done by polishing parallel to the crosses, stopping just before reaching them, so leaving some Si present. Fig. 2 shows the top view microscope image from the sample, taken with the MFI system.

The sample was tilted to expose the cross-section and the probes were again placed on Cross 1 (0 V) and 3 (5 V), now probing from the side. Fig. 3a indicates the position of the RDL-crosses at the top Si surface on which the probing is done. Fig. 3b shows an optical image of the X-section. The probes are visible at the top side. The thinned Si, glue and carrier wafer are also visible. The TSVs in the thinned Si are not visible in this optical image, they are covered by Si. Fig. 3c shows the current density image from MFI. Black arrows indicate the direction of

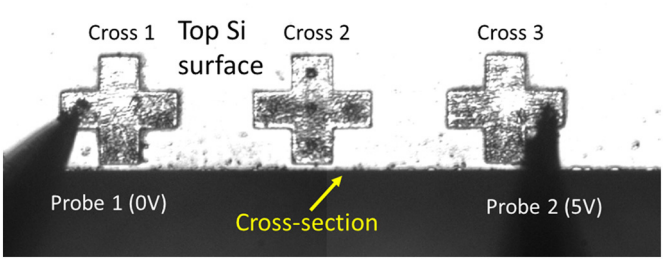

Fig. 2. Microscope image from the top of the polished sample. Probes are placed on Cross 1 and Cross 3.

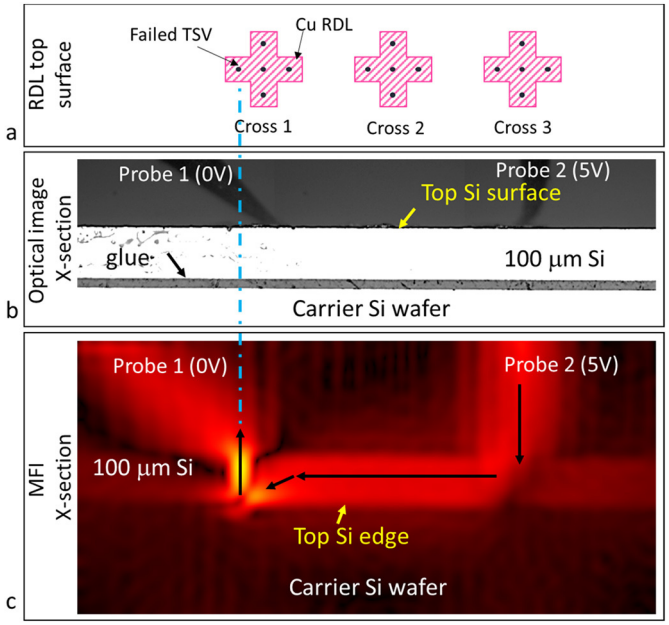

Fig. 3. a. The position of the RDL-crosses at the top Si surface on which the probing is done. b. Optical image of the X-section. c. MFI measured current density image on the cross-section. (For interpretation of the references to color in this figure, the reader is referred to the web version of this article.)

the current flow. The current density is denoted by color, from bright yellow (higher current density) to lower density (red), to black, denoting no current or within noise level. At the 5 V probe, the injection point, a weak broad current path is visible pointing to the fact that current distributes rather uniformly through the whole conducting structure, the RDL cross and then the different TSVs. Also in the thinned Si, the signal is weak and visible across the full width, pointing the presence of the leakage path. But near probe 1, the current density is higher (brighter) both near the bottom of the thinned Si and along a vertical line in the Si, that corresponds to the TSV that contains the fault. Note that because the current accumulates through the failure and into a single TSV, the current density is higher (bright yellow in

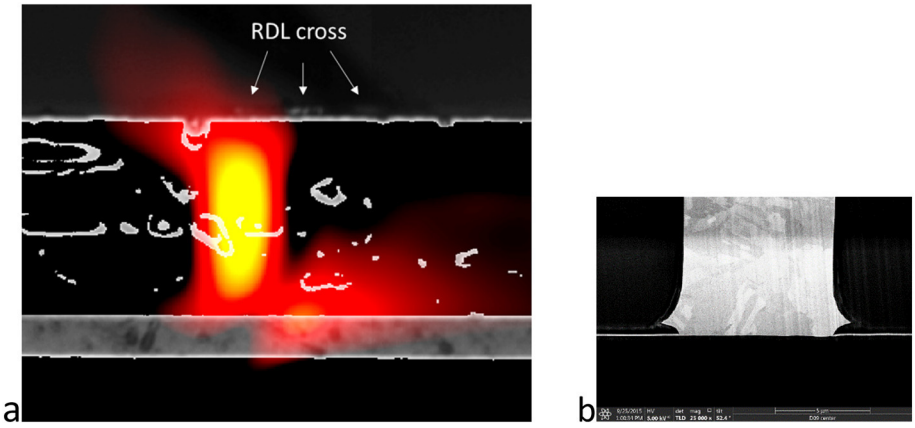

Fig. 4. a. MFI scan focusing on the position under cross 1. b. Cross-section MCI image showing the breakdown position and current leakage path between two TSVs. (For interpretation of the references to color in this figure, the reader is referred to the web version of this article.)

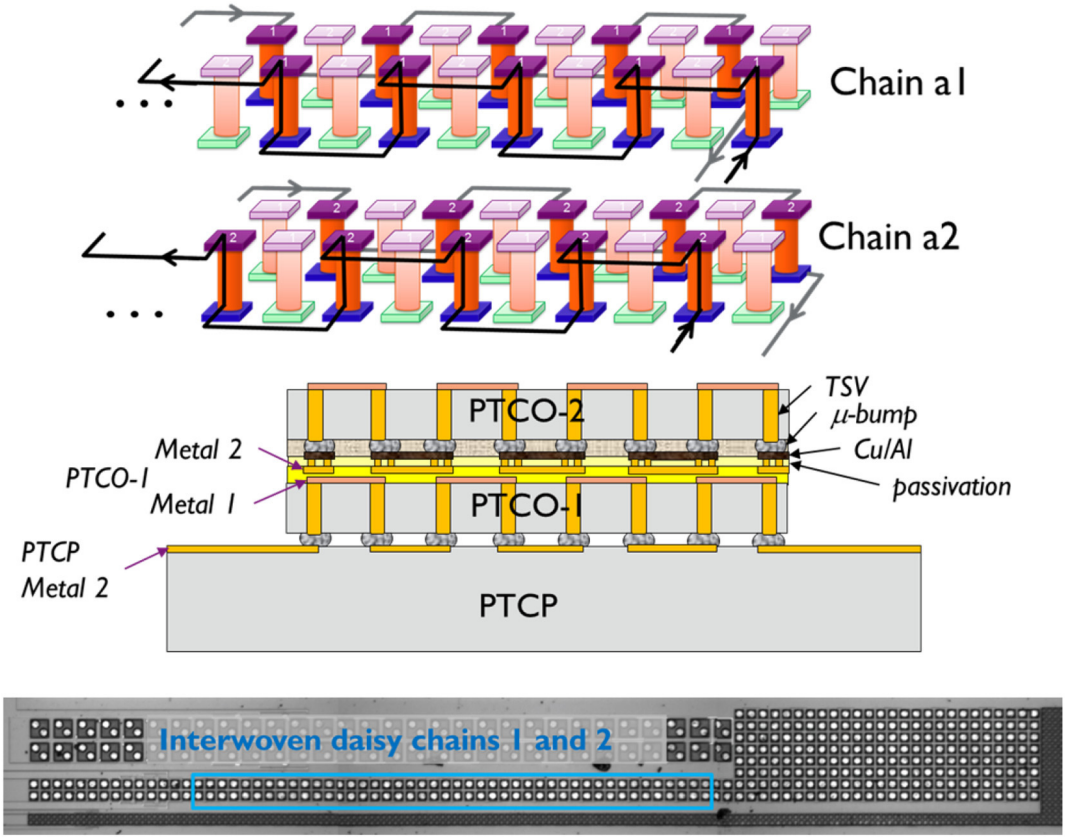

Fig. 5. Top: Schematic picture of interwoven daisy chain and test sample consisting of a stack of 3 chips. Bottom: top microscopy image of the interwoven daisy chain.

Figs. 3 and 4 than when it distributes over the 5 TSVs, as at the other probe point and the Si). These results demonstrate that MFI on a cross-section sample is indeed possible. Part of the current runs through the 5 TSVs of Cross 3, which is the reason that a weaker signal is seen at that position. But near Cross 1, the current only flows through one of the 5 TSVs, explaining the higher density (brighter image). The blue dashed line, comparing the position of this TSV with the position of Cross 1, indicates that this is the left TSV of this Cross. This is confirmed in Fig. 4a, showing an overlay MFI - optical image in that region. The metal of the RDL cross is visible, especially the centre part (which is closer to the cross-section edge). The bright MFI image corresponds with the location of the TSV at the left side of the cross. A FIB cross-section at the bottom of this TSV, shown in Fig. 4b, shows that this TSV had notching near the bottom, causing a high local electrical field and thus local breakdown of the liner. This was caused by a processing related problem at the bottom part of the TSVs.

3. Opens in TSV daisy chains

TSV daisy chains are often used during 3D technology development to control processing and stacking. In our test samples, these daisy chains consist of two interwoven arrays, a1 and a2, as shown in Fig. 5, top. In one failure case, an open was detected in one of these chains running in the central chip of a stack of 2 (PTCO-1, Fig. 5, center). The question raised whether magnetic field imaging, using radio-frequency (RF) space domain reflectometry (SDR) [3] can be used to locate the

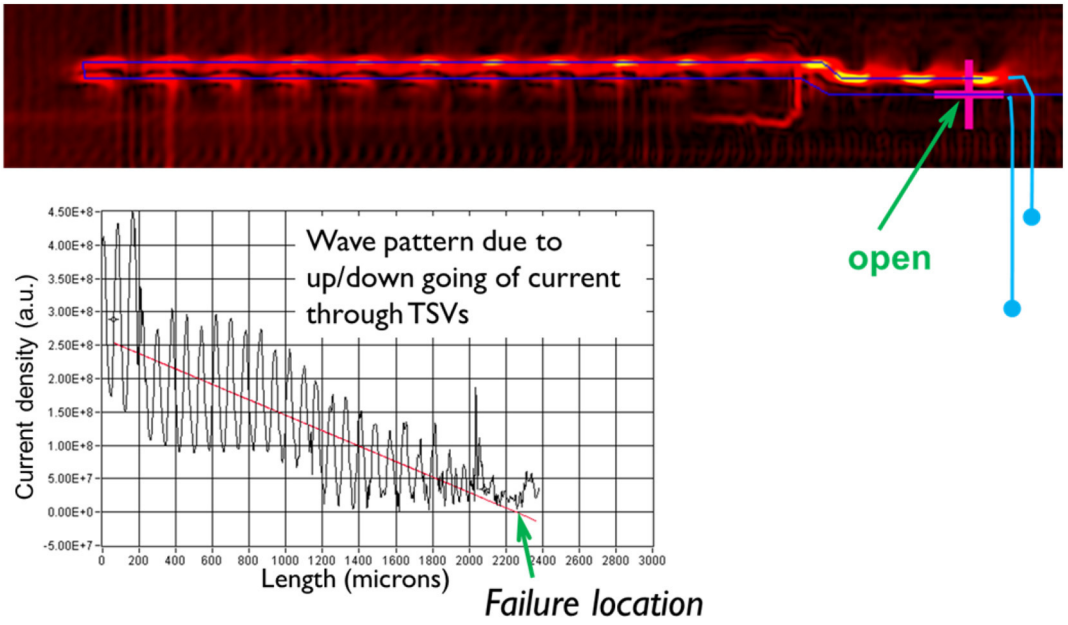

Fig. 6. Top: Current path obtained by MFI. Bottom: Estimation of failure location from the current decrease.

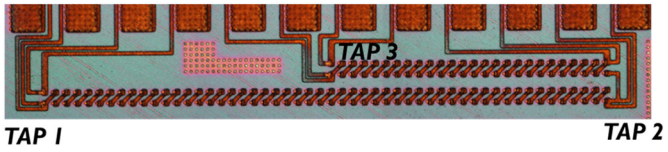

Fig. 7. Optical microscopy image of the TSV-daisy chain test structure.

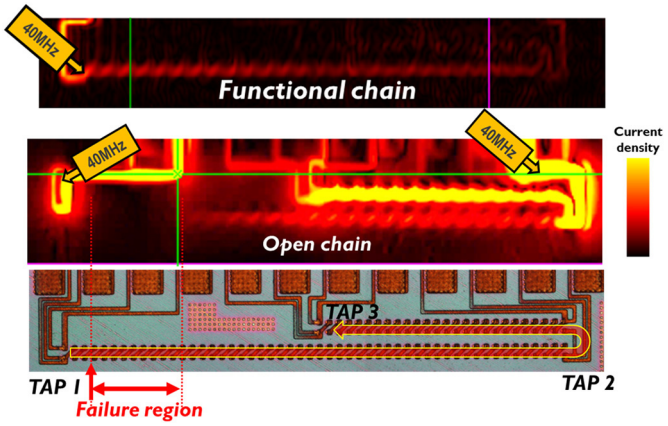

Fig. 8. Top: Current path obtained by MFI on a functional chain. Bottom: MFI image of a defective chain.

position of such an open.

SDR is based, as time-domain reflectometry and similar techniques, on the effect of impedance changes to injected signals of high enough frequency. The open reflects the incident signal, generating a standing wave on one side of the open while vanishing at the other. By spatially mapping the magnetic field associated with the reflected signal and finding where it goes to zero, pinpointing the location of the open is possible.

As shown in Fig. 6, a clear MFI signal was detected in the chain. The current path runs from the right top 2, to the left and comes back to the right along the bottom, i.e. the injected RF signal travels through the full daisy chain, decaying in intensity towards the open location where it should vanish [3], stopping close to the first TSV, indicating that the open is likely located there. This could not be confirmed (sample loss).

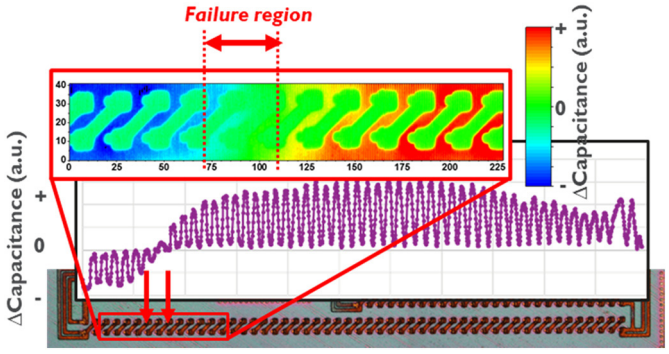

Fig. 9. LICA result on a defective chain.

In a second experiment, both MFI and LICA, which stands for light-induced capacitance alteration [8], were applied to find the location of open failures in TSV daisy chains. LICA is a scanning laser-based technique, which detects light induced changes in the depletion capacitance between the Si substrate and TSVs or between different TSVs where the Si substrate acts as an electrical coupling medium. The purpose of this experiment was to investigate how both techniques compare when applied on the same structure (but different dies on a common wafer), and to prove with physical FA that they indeed can detect opens. Since the first LICA demonstration, reported in [8], we have improved the measurement scheme evolving from a single-ended capacitance measurement towards a fully differential measurement. This configuration has enabled us to increase the detection sensitivity, and hence reduce the measurement time allowing us to obtain 2D image scans (instead of 1D line scans).

A microscope image of the test structure is shown in Fig. 7. It contains two interwoven TSV daisy chains, which can be tested at three locations (TAP 1, 2, 3). The TSVs are 5 × 50 μm in size, separated by a pitch of 20 μm, and interconnected by aluminium and copper metallization segments at the wafer frontside and backside, respectively. Each chain contains 78 TSVs. Electrical probing was performed on the RDL pads fabricated on the wafer backside. An electrical open with a resistance greater than 100 MΩ was detected between TAP1 and TAP2.

The structure was analysed using MFI and LICA. Fig. 8 (top) shows the MFI measurement result performed on a functional chain and

(bottom) on the defective chain. In the functional chain, an RF signal was observed along the full length of the chain indicating that all TSVs are electrically connected. For the defective chain, we observed a region without a signal, indicating electrical interruptions in the chain. By performing the measurement with RF signal injection at both chain terminals, it was found that the open position must be located close to TAP 1, and that the chain has at least two defects separated by 180 μm (i.e. the width of the region with no MFI signal). It must be noted that an impedance difference between the functional and failing samples results in different coupling of the RF signal to other adjacent circuits. For this reason, there are signals visible in the failing sample that are not (or not so evident) visible on the functional sample. Focus must be kept in comparing the difference between RF signal propagation along the TSV daisy chain (TAP1-TAP2-TAP3 connection). Through optical inspection of the wafer backside at the detected defective region, we could attribute the failures to a backside metal layer misalignment and confirm that physical defect locations are in agreement with the MFI data and indeed are open failures.

Next, a similar sample was analysed using LICA. Fig. 9 shows the LICA performed by simultaneously measuring the electrical capacitance of both chain terminals with respect to the Si substrate. The waveform in purple represents the LICA signal for the laser scanned across the length of the chain, from TAP 1 towards TAP 2. Due to the differential measurement configuration, the laser induced change in electrical capacitance can either have a negative or positive amplitude, depending on which side the laser spot is positioned with respect to the defect site. With the laser spot positioned towards the left site of the defect, a negative change in electrical capacitance is induced, whereas the opposite occurs with the laser spot on the right side of the defect. When the laser is focused at the defect site, the LICA signal is at zero amplitude, as the light-induced charge induces an equal change in both capacitance meters connected at TAP1 and TAP2.

Performing a high resolution 2D scan (shown in multi-color) allowed us to more accurately pinpoint the defect site. Similarly, as the case for the MFI sample, the open failure is located in the same region close to TAP 1. These results indicate that both techniques can be used to find open locations in TSV daisy chains. The spatial resolution of LICA seems higher than the one of MFI. On the other hand, LICA needs access of the laser to the Si substrate in order to be applicable, while MFI does not need optical access. This makes both techniques complimentary. Regarding measurement time, the 1-D LICA linescan needed ~20 min., whereas the MFI measurement could be performed typically in about 40 s.

4. Conclusions

This paper discussed TSV failure analysis cases involving two different defects: a leakage path between groups of TSVs covered with RDL metal, and opens in TSV daisy chains. The failures were detected using known failure analysis techniques, MFI and LICA, but either in a non-conventional way (cross-section) or for the first time on this kind of samples. In all cases the failure locations were successfully identified.

Declaration of competing interest

The authors declare that they have no known competing financial interests or personal relationships that could have appeared to influence the work reported in this paper.

Acknowledgements

The authors thank the 3D team of IMEC for providing the samples, and the IMEC partners for support and discussions. We thank J. Gaudestad, E. Talanova and A. Jeffers for all the help with setting-up the MFI experiments at Neocera, and Daisuke Kosemura for the sample preparation.

References

[1] E. Beyne, IEEE Des. Test 33 (3) (2016) 8–20.
[2] I. De Wolf, et al., IEEE Trans. Comp. Pack. Manuf. Techn. 8 (5) (2018) 711–718.
[3] D. Vallet, Electron Device Failure Anal. 16 (4) (2014) 26–34.
[4] A. Orozco, Magnetic field imaging for electrical fault isolation, Electronic Device Failure Analysis Desk Reference, 7th ed., 2019 (ISBN: 9781627082457).
[5] F. Altmann, et al., 3D localization of liner breakdown within Cu filled TSVs by backside LIT and PEM defocusing series, Proc. 43rd Int. Symp. Test. Failure Anal. (ISTFA), Pasadena, USA, 2017, pp. 19–24.
[6] A. Orozco, et al., 3D fault isolation in 2.5D device comprising high bandwidth memory (HBM) stacks and processor unit using 3D magnetic field imaging, Proceedings of the 42nd International Symposium for Testing and Failure Analysis, 2016.
[7] A. Orozco, et al., Non-destructive 3D Failure Analysis Work Flow for Electrical Failure Analysis in Complex 2.5D-Based Devices Combining 3D Magnetic Field Imaging and 3D X-ray Microscopy, Porc. 42th Int. Symp. Test. Failure Anal. (ISTFA) (2018).
[8] K.J.P. Jacobs, et al., Light-induced capacitance alteration for non-destructive fault isolation in TSV structures for 3-D integration, Proc. 42nd Int. Symp. Test. Failure Anal. (ISTFA), 2016, pp. 418–442.